

This item was submitted to [Loughborough's Research Repository](#) by the author.
Items in Figshare are protected by copyright, with all rights reserved, unless otherwise indicated.

A novel inertial positioning update method, using passive RFID tags, for indoor asset localisation

PLEASE CITE THE PUBLISHED VERSION

<https://doi.org/10.1016/j.cirpj.2021.10.006>

PUBLISHER

Elsevier BV

VERSION

VoR (Version of Record)

PUBLISHER STATEMENT

This is an Open Access Article. It is published by Elsevier under the Creative Commons Attribution 4.0 International Licence (CC BY 4.0). Full details of this licence are available at: creativecommons.org/licenses/by/4.0/

LICENCE

CC BY 4.0

REPOSITORY RECORD

Hayward, Steven, Joel Earps, R Sharpe, Kate Van-Lopik, J Tribe, and Andrew West. 2021. "A Novel Inertial Positioning Update Method, Using Passive RFID Tags, for Indoor Asset Localisation". Loughborough University. <https://hdl.handle.net/2134/16998787.v1>.



A novel inertial positioning update method, using passive RFID tags, for indoor asset localisation

S.J. Hayward*, J. Earps, R. Sharpe, K. van Lopik, J. Tribe, A.A. West

Loughborough University Wolfson School of Mechanical, Electrical and Manufacturing Engineering, UK

ARTICLE INFO

Article history:
Available online xxx

Keywords:
Asset Tracking
Dead Reckoning
Indoor Location
Indoor Navigation
Multiple-sensor systems
RFID
Sensor applications
Sensor data fusion

ABSTRACT

The benefits of the fourth industrial revolution are realised through accurate capture and processing of data relating to product, process, asset and supply chain activities. Although services such as Global Positioning Services (GPS) can be relied on outdoors, indoor positioning remains a challenge due to the characteristics of indoor environments (including metal structures, changing environments and personnel). An accurate Indoor Positioning System (IPS) is required to provide end-to-end asset tracking within a manufacturing supply chain to improve security and process monitoring. Inertial measurement units (IMU) are commonly used for indoor positioning and routing services due to their low cost and ease of implementation. However, IMU accuracy (including heading and orientation detection) is reduced by the effects of indoor environmental conditions (such as motors and metallic structures) and require low-cost reliable solutions to improve accuracy. The current state of the art utilises algorithms to adjust the IMU data and improve accuracy, resulting in error propagation. The research outlined in this paper explores the use of passive RFID tags as a low cost, non-invasive method to reorient an IMU step and heading algorithm. This is achieved by confirming reference location to correct drift in scenarios where magnetometer and zero velocity updates are not available. The RFID tag correction method is demonstrated to map the route taken by an asset carried by personnel in an indoor environment. The test scenario task is representative of warehousing and delivery tasks where asset and personnel tracking are required.

© 2021 The Author(s).
CC BY 4.0

Introduction and motivation

Manufacturers have started investing in hardware, software and global networking systems to further the advancement of the Internet of Things (IoT) [1]. The German government heralded this as the next industrial revolution and termed the research and development to achieve this global network of intelligent products and processes “Industrie 4.0” [2]. Worldwide industrial initiatives are aiming to bring cross platform communications to the shop floor, e.g. in the United Kingdom the “Future of Manufacturing” movement, in the US the ‘Advanced Manufacturing Partnership’ and in Japan ‘The 5th Science and Technology Basic Plan’ [3]. The vision for these Smart Industries is to include intelligent networks comprising Cyber-Physical Systems (CPSs), which link the physical world and information communication technology (ICT) services to create systems that can control, maintain and analyse capabilities and performances to respond to changes in production [1]. One of the

most critical requirements is accurate positioning data to provide contextually relevant, location-based services [4]. Two of the pillars for this revolution are to know one’s location and the location of objects in the surroundings (i.e. the location of one object with respect to others). These data are critical to a CPS to ensure autonomous actions can address the frequently changing environment and material handling requirements within a factory and its supply chain. Many localisation systems require additional infrastructure and anchor nodes that may require dedicated servers and databases. Changes to infrastructure adds cost and implementation complexity, which are recognised as barriers to adoption of Industry 4 technologies, particularly in small/medium scale enterprises with limited resources [5]. Minimising the costs and barriers to adoption of CPS technologies highlights the need for a low cost, low infrastructure impact system.

The deployment of an increasing number of communicating and intelligent devices (i.e. 35 billion in 2021 [6]) increases the viability of an indoor location system which utilises the capabilities of such devices. Location methods can be differentiated as suitable for indoor localisation and outdoor localisation. Both methods rely on communication between a receiver node at the object of interest and

* Corresponding author.
E-mail address: s.hayward@lboro.ac.uk (S.J. Hayward).

several fixed points [7]. An Indoor Positioning System (IPS) uses information gathered from one or more devices to create a navigation system to locate objects or people in indoor environments [8]. The IPS provides the data for any Indoor Location Based Service (ILBS), such as navigation or equipment tracking within an indoor environment [9]. The predicted ILBS market was expected to be worth \$10bn by 2020 [9].

In addition, manufacturers are under increasing pressure to improve their efficiency and productivity and minimise loss and waste. Traceability of assets within the supplier premises often has limited granularity, with localisation given on a room-by-room basis, identifying object passage through gateways with no visibility between these gateways. This loss of visibility presents possible vulnerabilities for stock loss, also known as ‘shrinkage’, in industry [10]. One common example of stock loss is theft, which may be committed internally (by employees) or externally (for example by a customer or vendor) [10]. In the consumer goods domain shrinkage accounts for 2.41% of the sector turnover value, equating to €24 million in 2003 [11]. Knowing the location of mobile equipment and assets in manufacturing is a key part of increasing efficiency and productivity, since misplaced equipment can lead to lost time spent finding parts, delaying production [12]. Several examples of the four common methods of record discrepancy: (i) stock loss, (ii) transaction error, (iii) inaccessible inventory, and (iv) incorrect product identification [10].

The asset supply chain can be considered as several links between supplier and consumer which are often delivered by a third-party courier. The key asset tracking points within these supply chains are illustrated in Fig. 1 and can be summarised as: (i) Storage of assets, (ii) Asset relocation within a factory (iii) Loading of assets for transport, (iv) Asset transport to the customer and (v) Physical delivery to the customer.

A loss of assets may also refer to the loss of digital assets alongside the physical ones. The nature of ubiquitous connectivity within IoT and Industry 4 systems brings an increased need for improved traceability since a loss of assets would additionally lead to a loss of the data contained within it. Risk mitigation has gained recognition as an increasingly important part of CPS and IoT design

due to the increasing number of IoT devices that are interconnected each year [13]. Additionally, there is a need to consider data privacy and protection in order to comply with legislation and ethical system development (e.g. the European General Data Protection Regulation (GDPR) and the UK implementation of this as the Data Protection Act (DPA) 2018). The DPA guidelines Section 57 deals specifically with protection of data in transit/transport requiring “Data protection by design and default”, the article states “Each controller must implement appropriate technical and organisational measures for ensuring that, by default, only personal data which is necessary for each specific purpose of the processing is processed” [14]. The data protection measures apply to the data’s availability requiring that, to the best of the holder’s ability, data be protected from malicious damage and access. When transporting data holding assets, knowing the location and security status of the media contributes towards section 57 compliance, mitigating risk and associated costs of data loss, in addition to reputational damage, failure to comply with section 57 could lead to fines up to 4% of a firm’s annual global turnover or €20 Million [15]. Knowing the location of such assets can highlight unauthorized movement indicating possible intention of misuse, enabling supervisors to address arising issues and reduce the risk of data loss. Fig. 2 illustrates how increased localisation granularity is likely to improve stock loss due to theft and transactional errors, primarily stemming from incorrect asset logging.

The goal of the research presented in this paper was to develop a localisation solution for tracking assets carried by personnel indoors, a scenario in which zero velocity updates are not possible i.e. the asset is carried by hand [16] and strong electromagnetic fields make heading determination from a magnetometer unfeasible such as in a factory environment where an abundance of ferromagnetic materials degrade heading estimation [9]. Furthermore, to support deployment in industry for a variety of settings, budgets and environments, the solution must minimise the impact on current infrastructure by allowing for easy deployment, utilising low-cost equipment requiring minimal maintenance.

The structure of this paper is as follows: Section II summarises academic literature related to the system and IPS proposed

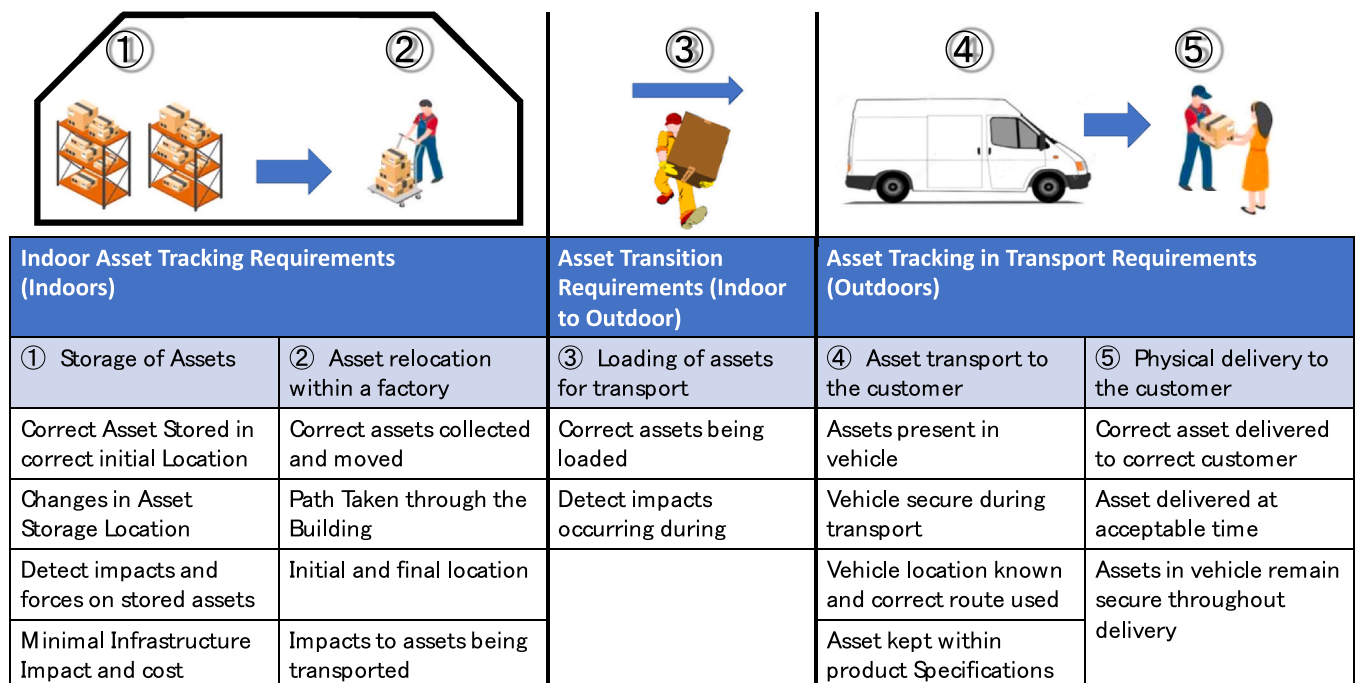


Fig. 1. Key stages of an asset delivery process from supplier to customer and the important aspects at each stage.






Stage of Delivery	① Storage of Assets	② Asset relocation within a factory	③ Loading of assets for transport	④ Asset transport to the customer	⑤ Physical delivery to the customer
					
(i) Stock loss	<ul style="list-style-type: none">• <u>Theft of assets</u>• Damage due to incorrect storage condition	<ul style="list-style-type: none">• <u>Theft of assets</u>• Damage during relocation (e.g. impacts/ dropping)	<ul style="list-style-type: none">• <u>Theft of assets</u>• Damage during loading (e.g. impacts/ dropping)	<ul style="list-style-type: none">• Damaged in transit (e.g. shifting)	<ul style="list-style-type: none">• Damage at delivery (e.g. dropped)
(ii) Transaction error	<ul style="list-style-type: none">• <u>Incorrect storage location recording</u>• <u>Incorrect logging of inventory change</u>	<ul style="list-style-type: none">• <u>Incorrect new location recording</u>• <u>Failure to update new location</u>	<ul style="list-style-type: none">• <u>Incorrect logging of inventory change</u>• <u>Incorrect asset loaded</u>	<ul style="list-style-type: none">• N/A	<ul style="list-style-type: none">• <u>Incorrect logging of product handover</u>
(iii) Inaccessible inventory	<ul style="list-style-type: none">• Poor storage planning			<ul style="list-style-type: none">• N/A	
(iv) Incorrect product identification	<ul style="list-style-type: none">• Product ID and Physical Product Mismatch				

Fig. 2. Possible opportunities for asset record discrepancies, highlighting areas where localisation granularity would be beneficial.

application. Sections III and IV define system concept and hardware respectively. Sections V summarises the limitations of using RFID technology. Section VI details the collection, preparation, and analysis of inertial measurements to determine location. The two techniques have been combined using sensor fusion to create a prototype system discussed in section VII. Finally, Section VIII presents the findings of this research, the effectiveness of the proposed system, implications for practitioners and presents future work.

Related work and theory

The indoor location methods identified in the academic literature can be considered in three categories: (i) Network based systems – using information within wireless network signals to determine location, (ii) Inertial based systems – using self-contained sensors to analyse motion to determine location and (iii) Hybrid systems – combining two or more approaches [8,9,17]. Several methods that are being used to improve the accuracy of indoor positioning systems were identified in the literature (based on information from [8,9,17]) shown in Fig. 3.

To reduce the need for infrastructure changes, inertial based systems have been explored, often in conjunction with RF techniques, by using the responses from IMUs to perform Dead Reckoning [7,18,19]. Micro Electro Mechanical Systems (MEMS) have increased the availability of low cost microsensors which can be used to detect environmental changes by measuring mechanical, thermal, magnetic, chemical or electromagnetic information [20]. An IMU is a combination of microsensors, commonly containing three accelerometers measuring linear accelerations acting on an object with a local frame of reference oriented perpendicular to one another, three gyroscopes to measure angular speed about these axes and a magnetometer to detect ambient magnetic fields associated with the same three axes. Location determined using this technology is determined based on previously known locations, the direction travelled and distance travelled in that direction [21]. Typical accuracies quoted are to 0.3–1.5% of the path travelled [9].

Some IMUs include an altimeter to detect external air pressure giving nine degrees of freedom and current elevation [22]. Critically, IMUs can meet requirements for scalable deployment using low cost sensors (e.g. LSM6DS3TR ST Microelectronics costs £2.64 [23]) for estimating position whilst being self-contained, without the need of

supporting infrastructures [3]. Dead reckoning can be achieved with an IMU using either the *Integration* or *Step and Heading* techniques [9]. The *Integration* technique is where the sensor is mounted along three orthogonal axes to the rigid body to be tracked, resulting in, theoretically, no relative motion so the measurements can be directly identified as the assets motion [24]. The angular speed is integrated to give the heading used to orientate the measured accelerations, which following corrections for gravitational acceleration, can be integrated twice to get distance travelled [9]. The process is shown in Fig. 4 and the calculation for speed and direction travelled are given in Eqs. (1) and (2).

Distance Travelled from acceleration measured by an IMU [25] $\mathbf{x}(t)$

$$= \mathbf{x}(0) + \int_0^t \int_0^t (\mathbf{a}(t) - \mathbf{g}) dt dt \quad (1)$$

Derivation of heading from angular speed measured by an IMU [25]

$$\theta(t) = \theta(0) + \int_0^t \omega(t) dt \quad (2)$$

\mathbf{x} = Displacement Vector \mathbf{a} = Linear Acceleration Vector θ = Heading Angle.

ω = Angular Speed about gravitational axis t = Time.

To remove the effect of gravity, the IMU data need to be transformed from the local or body frame to the global reference frame. To achieve this, gravity is used as the global Z-axis and the rotation operation (often expressed as a quaternion) which rotates the local Z-axis to the global Z-axis is applied to the IMU prior to double integration [26]. However, there are limitations to the successful use of IMUs in IPS. An issue with Inertial measurements is that all calculated movements are determined with respect to the initial start point, only allowing extraction of a relative path rather than a known position in the real world requiring initialisation [18,21]. In lower cost sensors some errors in the measurement can occur from influences such as: (i) Non-orthogonality – misalignment of the sensor axes in the IMU leads to partial measurement of the same components [27], (ii) Scaling – multiplicative errors such as sensors responding with 10% larger outputs the actual value [27] and (iii) Bias – adding constant offset values to the axes [27]. Unfortunately, the integration to obtain distance and angle leads to such errors propagating over time and any inaccuracies in the acceleration or angular speed causes the location to deviate quickly from the ground

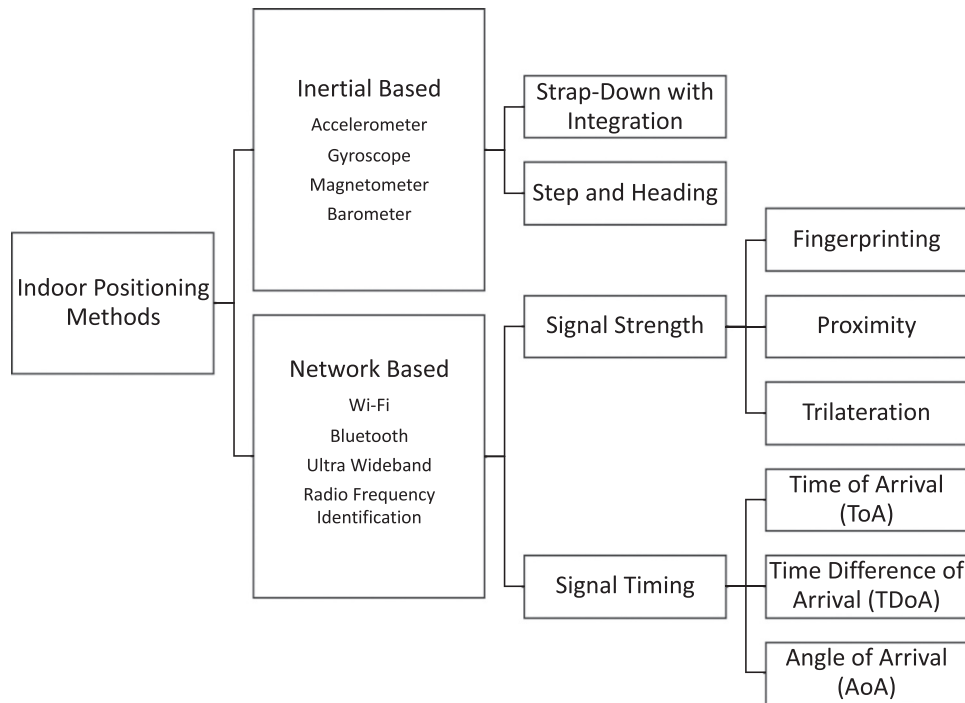


Fig. 3. Technologies commonly used to attempt to provide a solution to indoor localisation.

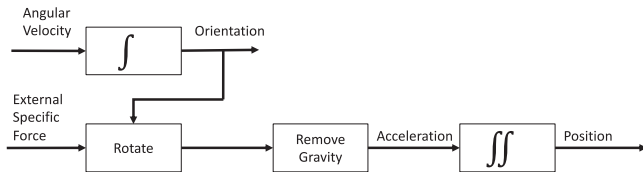


Fig. 4. Schematic for position estimation based on IMU readings redrawn from [25].

truth [9]. The alternative *Step and Heading* technique uses the acceleration response from the IMU to determine features of a step, with the obvious drawback that it is only valid for motions including steps or repetitive features within acceleration signatures. The location can then be calculated using the heading from Eq. 2 and an estimated step length to give the next location point [9]. Unlike the *Strap-Down* with integration method, *Step and Heading* errors propagate linearly, potentially reducing the error in estimation. However this technique when applied to items that are carried by humans is reliant on accurate step detection and stride length which may vary (typically set to 150–170 cm for an adult male [28]) adding an additional source of error or requirement for user interaction for calibration on each use.

Pedestrian dead reckoning (PDR) is a technique of great interest to researchers in the field of indoor positioning [8,9,17]. In dead reckoning, the error increases as a percentage of distance leading to inaccuracies of as much as several meters over 2 s as seen in Fig. 5. Sensor drift (in cheaper sensors the zero-g offset can be in the order of $\pm 1 \text{ m/s}^2$ [22]) and summation of errors over time require additional information (such as zero velocity conditions) in order to determine absolute position [21]. Researchers have attempted to develop multi-modal systems to address these issues by combining IMU dead reckoning with additional technologies [18,22]. For example Yoon et al. used dead reckoning as a guide when Global Navigation Satellite System (GNSS) signal was lost in an outdoor application [18]. Chen et al. supported proposed the use of an IMU with time of arrival (ToA) calculations using radio frequency and ultrasound pulses [22]. This approach was improved by a maximum a posteriori (MAP) algorithm reducing the mean error from 0.46 m

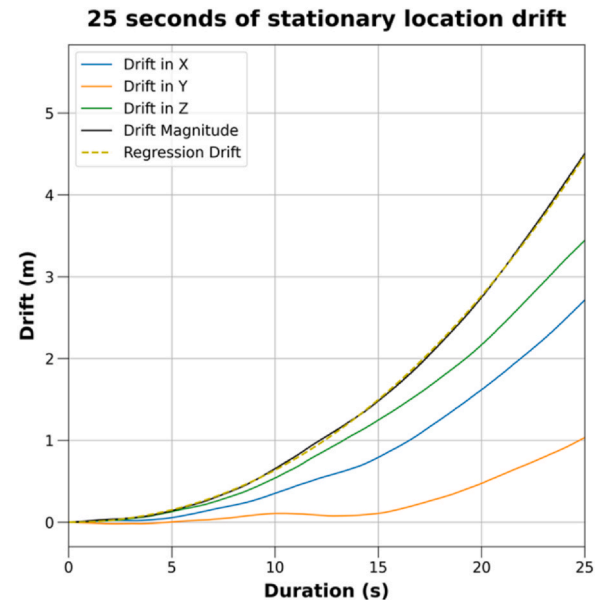


Fig. 5. Deviation of location calculated from sensors over time due to sensor offset and noise.

using ToA alone to 0.31 m over a path > 50 m within a room of dimensions 25 m by 8 m [22].

Haverinen et al. explored the use of IMU's magnetometer for magnetic field mapping, a technique relying on the disturbance of the earth's magnetic field due to ferrous structures and electronic appliances. These disturbances provide a static magnetic fingerprint which can be combined with a lookup table for the closest matching location to the measured fingerprint to determine localisation [29]. However this approach is likely to function poorly in a factory environment, due to varying magnetic fields induced by machinery in manufacturing processes (e.g. electronic motors) as magnetic fingerprinting is vulnerable to external magnetic perturbations [30].

Network based systems commonly use Received Signal Strength (RSS) of radio signals to estimate location or to support location information extracted from inertial measurement units (IMUs) and magnetic field mapping [31]. Radio frequency identification (RFID) technologies are widely used to collect location data [32], due to being low cost (complete systems obtainable for <£100) and utilising radio-wave data communication [33]. The technique uses reference tags attached to objects of interest and the power of the response received from the reference tag in dB is recorded. This RSS is used to estimate an object's location using a power curve in which the RSS is typically proportional to the square of the distance from the tag. Several studies used RSS indicators as a variable for identifying location [34–36]. The technologies used included radio frequency emitters (e.g. RFID tags, Bluetooth Low Energy (BLE) beacons or Wi-Fi routers [9]). The cost varied from £0.01 to > £100 per beacon depending on the technology [37]. In addition to set up costs, through life costs such as maintenance and adaptations to the infrastructure for implementation can be a significant deterrent for industrial adoption. Accuracy of systems utilising RSS for localisation presented positional errors of 1.4–3 m [9]. However, radio signals suffered from multipath errors due to Non-Line of Sight (NLOS) reflections causing signal attenuation (i.e. a reduction in RSS) due to absorption, amplification (i.e. an increase in RSS) or attenuation due to signal scattering from environmental objects. These variations were reported to cause deviation from the expected response model, severely affecting location estimation and uncertainty [33]. Until recently cellular networks were poor candidates for IPS, however, with the introduction of 5 G, emerging technology may make use of cellular networks [9] with research reporting decimetre accuracy with line of sight when using time of flight (ToF) measurements [38]. The limitations of 5 G are that ToF is impacted by NLOS conditions [38] and, at the time of writing, 5 G equipment was expensive, involving significant infrastructure impact for installation, therefore, although 5 G shows potential for future systems, it was considered out of scope for this work.

Many algorithms have been developed to improve the reliability and accuracy of RSS methods, by positioning reference tags in a grid format. Two such approaches can be found in LANDMARC which utilises nearest neighbour conditions to estimate a target location [33] and VIRE which sub-divides each group of 4 reference tags into $N \times N$ elements to determine location based on a weighting of the nearest neighbours [33]. The main drawback of these systems is that many nodes (e.g. 1 tag per m^2) are required to improve accuracy which also increases the algorithm complexity and implementation costs. However, the accuracy of such algorithms in harsh environments, such as highly metallic factories with significant radio frequency noise generators, has not been tested. These harsh environment scenarios are of paramount importance for manufacturing deployments due to their prevalence. This is particularly important when using RFID methods since metallic objects greatly affect the radiation efficiency and gain of RFID antennas, reducing reading distance by > 40% of the tag specification [1] and reducing signal strength by up to 60% [39].

The use of a network of RFID tags with unique Electronic Product Code (EPC) values could be used to indicate known positions in a real-world space, allowing a link between path travelled and real-world position on a floorplan. A similar approach has been reported in [40] where active (i.e. tags which broadcast continually using a battery [41]) RFID tags were used. In addition the authors utilised a foot mounted IMU which allowed the use of zero velocity updates (ZUPTs) in the identification of steps (i.e. identification of the stance phase [42] as no motion) which is not a possibility for tracking non-human assets since assets transported by stillages, forklift trucks or automated guided vehicles and not carried by humans and do not have a regular zero velocity position in their patterns of motion [16]. In addition, the use of active RFID tags requires additional

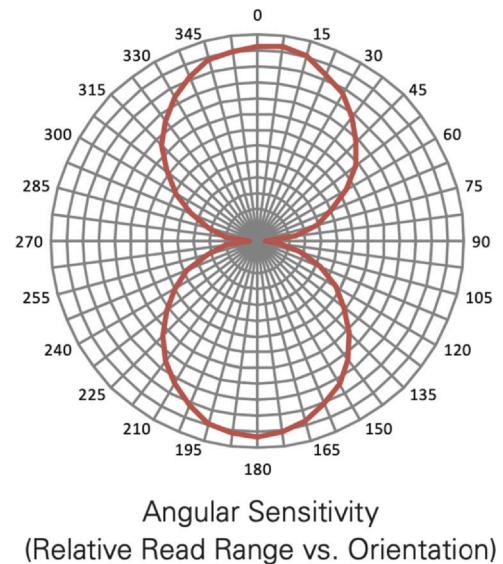


Fig. 6. Angular impact on sensitivity and read range for the ALN-9640 UHF RFID tag [43].

maintenance and cost as the price for an active RFID tag is often tens to hundreds of dollars depending on functionality and can require replacement batteries every 1–12 months depending on broadcast rate and power [41]. Passive RFID tags can cost as low as a few pence and require no maintenance or batteries to continue to function [41], making them suitable for an inexpensive method of deploying an IPS. Passive RFID can be used in conjunction with IMUs. The relative movement of a directional antenna and passive RFID tags induces an increase and reduction of signal strength dependent on field alignment of the antenna to the tag (see Fig. 6). This response could be used as an update point for a dead reckoning indoor positioning system using an IMU by determining footsteps in a given direction and updating location based on observation of fixed RFID tags at known locations.

To track an object carried by a human via dead reckoning, the IMU would need to be attached to the object which whilst being carried, exhibits no repeatable zero velocity conditions. Thus, the ZUPT feature extraction technique cannot be used to mitigate the drift integration discussed in Section II. Due to this the *Strap-Down* method with a step and heading approach was used to determine asset motion and location. The “steps” were detected using a combination of low pass (i.e. Butterworth second order filter for frequencies over 10 Hz) filtering to remove noise the accelerations in the Z-Axis and identifying changes in gradients in acceleration and zero crossings. The algorithm used for detecting steps will be discussed later in Section VI. The *Strap-Down* technique is supported by a network of RFID tags detected when a received signal strength indication (RSSI) was greater than a pre-determined threshold as discussed in Section V.

The novelty in this method lies in the use of feature extraction from passing Passive RFID tags in a location where a magnetometer cannot be used to obtain a heading. The method utilises the relatively short range of passive RFID tags (i.e. a maximum stated range of < 10 m [41]), to enable more accurate location updates than similar methods which use the variation in RSSI to determine position in order to reduce the variability in the update of the inertial unit's position. It is noted however, that the location of the RFID tags needs to consider the material of its surroundings since metallic surfaces greatly reduce the read range of RFID tags therefore RFID tags will be positioned with sufficient clearance of metal objects where practical. To mirror the situation where larger items are being carried around a workspace, a regular tote box container (i.e. HDPE container with

Table 1
Summary of technology approaches and corresponding accuracies for research and commercially available solutions utilising reviews from [9,44–48,49], with approximate hardware costs from [37,50–52].

System Technology	Cost (Antenna)	Cost (Receiver)	Infrastructure Impact	Receiver Power Consumption	Coverage	Scalability	Accuracy	Impact of metal interference	Line of Sight Needed	Signal Type	Limitation
Inertial System	≈ £15 – £30 +		None	Very Low	10 m ² – 2500 m ² +	High	0.8–2% of path travelled	Drift can impact error by > 0.5 m/s	No	Environmental /Physical Phenomena	Relative location only Sensor bias and noise
Wi-Fi	≈ £10 – £20	≈ £40 – £200 +	High unless already existing	Moderate	10 m ² – 2500 m ² +	High	0.4–5 m	Moderate	No	Radio Frequency (2.4 GHz or 5 GHz)	Ambient Interference Low accuracy Expensive if not installed
Magnetic System	≈ £5 – £10 +		None	Very Low	10 m ² – 2500 m ² +	High	2.5 m	High	No	Magnetic Field	Magnetic fields vary in changing environment Time consuming setup
Bluetooth LE	≈ £10 – £30		Moderate	Low	10 m ² – 1000 m ² +	Moderate	0.9–2 m	High	No	Radio Frequency (2.4 GHz)	Impacted by ambient interference Low Accuracy
Ultrawideband	≈ £10 – 200		Low-Moderate	Low-Moderate	10 m ² – 400 m ²	Low	0.3 m – 0.5 cm	Moderate	No	Radio Frequency (3.1–10.6 GHz, 500 MHz bands)	High power consumption High infrastructure impact
UHF RFID (Passive)	≈ £100 – £250 + £50 – £100 per antenna	≈ < £0.05	Low	Low	10 m ² – 1000 m ² +	Moderate	1–5 m	High	No	Radio Frequency (860–960 MHz)	High Antenna and Reader cost Severe impact of metal
UHF RFID (Active)	≈ £100 – £250 + £50 – £100 per antenna	£10 – £50 +	Moderate	High	10 m ² – 1000 m ² +	Moderate	0.1–1 m	Moderate	No	Radio Frequency (860–960 MHz)	Metal interference High unit cost Frequent maintenance
Ultrasound	≈ £5 – £25	≈ £5 – £25	Low-Moderate	Moderate	10 m ² – 2500 m ² +	High	0.1–0.6 m	Moderate	Yes	Ultrasonic (20 kHz)	Line of sight Ambient sound interference

dimensions 600×400×365mm) was fitted with an antenna and RFID reader in addition to an IMU mounted internally. A summary of the technologies and their corresponding attributes is shown in Table 1, derived from both academic and commercial applications. It should be noted the accuracy is dependent on the size of the area the system is deployed over. Although IPS technologies have been compared and contrasted in the reviewed literature [53,46,45], a single, preferred algorithm or technology combination has yet to be established. A preferred IPS system should provide large path coverage (which this paper will consider as > 50 m) minimal infrastructure impact (which this paper will consider as battery operated, or mains powered equipment attached to the building) and minimal cost and maintenance requirements (considered in this paper as infrastructure maintenance of no more frequent than 6 months). At present, no solution maintains acceptable accuracy (considered as a mean distance error < 1 m with a standard deviation of 0.5 m) [46] whilst meeting the identified requirements.

Methodology

From the limitations of individual technologies, it was clear that a multi-modal solution is required. Therefore, the proposed IPS approach combines the two technologies with the lowest infrastructure impact whilst maintaining the required accuracy from Table 1: (i) Inertial Measurements and (ii) passive RFID. The research outlined in this paper integrates a dead reckoning technique for tracking handheld objects using peak detection within a continuous recording of an RFID tag's RSS indicator to identify the strongest signal received. This provides the closest point and best alignment of the reader and the tag which could then be used as an update fiducial. The use of a system incorporating IMU's and passive RFID tags as an inexpensive and very low infrastructure impact is a novel approach to correcting IMU drift and inaccuracy over time whilst linking relative path to absolute location. A hardware architecture for a multimodal system to determine indoor location has been developed that can be used to build services such as traceability, observability, routing and building utilisation applications. This system results in advantages over other proposed systems due to the use of passive RFID tags positioned around the building, leading to little infrastructure cost and maintenance frequency (i.e. > 2 years). The use of a novel portable RFID reader transfers the system cost to the asset in place of the infrastructure.

This use of RFID passive tags was selected due to their longevity and low cost, minimal infrastructure impact from the use of a portable RFID reader. Additionally, these enable the transfer of costs and maintenance requirements from the infrastructure to the tracked item. Unfortunately, at larger distances (e.g. > 2 m) variability in the RSS of passive ultra-high frequency (UHF) RFID tags make distance measurements error prone and unreliable when using RSS alone [54].

Based on the limitations and benefits of each of the evaluated technologies, the proposed system was developed using an IMU with supporting RFID passive tags and tested in a real-world environment to simulate tracking in a warehouse and factory whilst minimising confounding factors and ensuring repeatability of the tests. The materials, protocol and evaluation of results are described in the following sections.

Hardware and testing setup

An illustration of the hardware for the developed system can be seen in Fig. 7. The IMU selected was a PMOD NAV development board with data collected by an Espressif ESP32-WROOM-32D [55]. Data were stored by a Raspberry Pi 3 [56] via the serial port. The IMU was located at a fixed orientation with respect to the handles of the box so the Z-Axis could be readily determined (i.e. the base of the

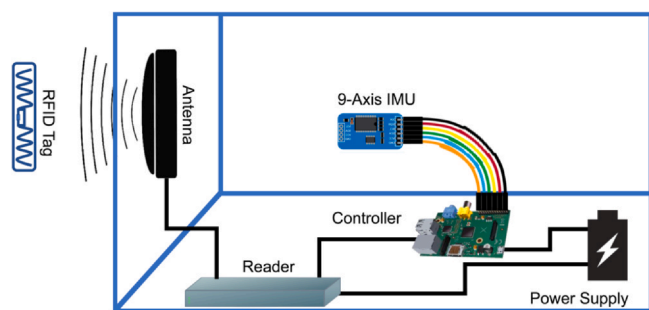


Fig. 7. IMU Box Setup With power supply and Controller board to orchestrate the data collection and RFID reader operations.

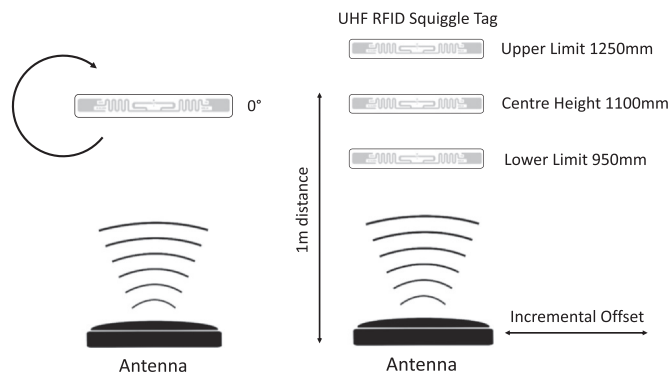


Fig. 8. Experimental setup for RFID tag rotation test (left) and Horizontal offset testing setup for antenna and tags (right).

box should be parallel with the ground plane). Similarly, the fixed mounting orientation enabled changes in direction to be extracted easily as positive changes in angular speed would correspond to a right-hand turn whilst negative changes in angular speed would correspond to a left-hand turn. The Raspberry Pi was also used to receive and record data picked up by the Alien ALR-8696-C Circular polarised antenna [57] through the Alien Reader ALR-9900+EMA [58] (from here referred to as the portable reader / antenna). This equipment was only to be used for proof of principal, smaller more accessible equipment would need to be used in future work and for an optimal solution. In addition, the power consumption of such equipment would need to be assessed to allow for a smaller power supply and a more discreet using, to be used for more practical applications.

The testing was conducted using a carrying tote equipped with RFID tags and reader, extracting features of walking motion from the carried IMU. The IMU location estimate was supported using location estimated from temporal features in addition to maximum RSSI value of the UHF RFID tags, positioned at known locations.

RFID capability testing

Position of the asset tags

To ensure the ideal orientations of RFID tags with respect to the portable reader, positioning of the tags on the tracked asset were analysed and the optimal placement was identified. The correct

positioning was evaluated through real world testing (see Fig. 8 (left)) with thirty readings of RSSI and angle of tag with respect to reader for a range of tags positioned 2 m away from the reader. The tests were repeated with each tag rotated by + 90-degree offsets in a clockwise direction. Each set of tests was repeated 3 times. Based on analysis of the results (see Section VIII – A) the antenna was positioned on the side of the box and tags aligned with the long side parallel to the floor to ensure the maximum opportunity for tag alignment.

Position of environmental reference tags considering personnel carrying item

To determine the effect of horizontal and vertical offset on the RSS of a tag and to ensure a peak feature could be identified by moving an antenna laterally with respect to a tag in addition to testing the effect of carry height of an asset, a stationary test was conducted with the RFID antenna positioned 1 m away from a wall where the tags were attached (see Fig. 8 (right)). Good manual handling technique suggests items carried by hand, should be carried with upper arms parallel to the torso and elbows at 90° [59], therefore the equipment carried would be approximately elbow height. Due to the nature of the RFID tag being located at a fixed location on a wall it was not possible to accommodate a range of heights for a varying population carry heights. In this case, the limits of elbow height were to be used, for a mixed male/female population, this dimension is 1100 mm with a range of ± 150 mm [60]. Therefore, the RFID tags for testing were located at an upper limit 1250 mm, centre point of 1100 mm and lower limit of 950 mm. The antenna was positioned at 1100 mm high so the results for each tag would then account for the likely range of person carry height. The test was repeated at 500 mm lateral intervals (with an 250 mm section nearer the tag) to identify what RSS values could be seen when parallel to the tag with the given offsets. The results of this test have been presented in Section VIII – A. This test resulted in a positional accuracy of ± 0.75 m within 3 standard deviations for a threshold value > 5000 RSSI. Hence for the RFID tag to be registered with the system, the minimum update frequency must be such that a single reading takes place within the 1.5 m window.

To confirm the correct functioning of the antenna and tags, a test was conducted (total duration 5 min) with the antenna pointing at an individual tag to determine the maximum rate at which the tag could be read. It was found the average sample rate of the system was 0.32 ± 0.1 s. A summary of the testing conducted is given in Table 2.

IMU step and heading detection

It has been reported in previous studies the average stride length of a 95th percentile adult male is between 150 cm and 170 cm (i.e. full walking cycle is from heel strike on one leg to heel strike on the same leg therefore 2 steps [42]) which yields step lengths of between 75 cm and 85 cm. In addition, the average walking speed was found to be 1.4 m/s [28]. Combining the average read rate with the average walking speed equates to a distance between reads of 0.45 ± 0.14 m, as shown in Equation 3.

$$\begin{aligned} \text{Distance} &= \text{Walking Speed} \times \text{Sample Rate} = 1.4 \times 0.32 \\ &= 0.45 \pm 0.14\text{m} \end{aligned} \quad (3)$$

Table 2
Summary of testing conducted.

Fixed Component	Variable Component	Variable	Increment	Measurement	Number of Tags
Antenna	Tag	Angle (°)	90	RSSI	1
Tag	Antenna	Horizontal Offset (mm)	500 (250 either side of centre)	RSSI	3

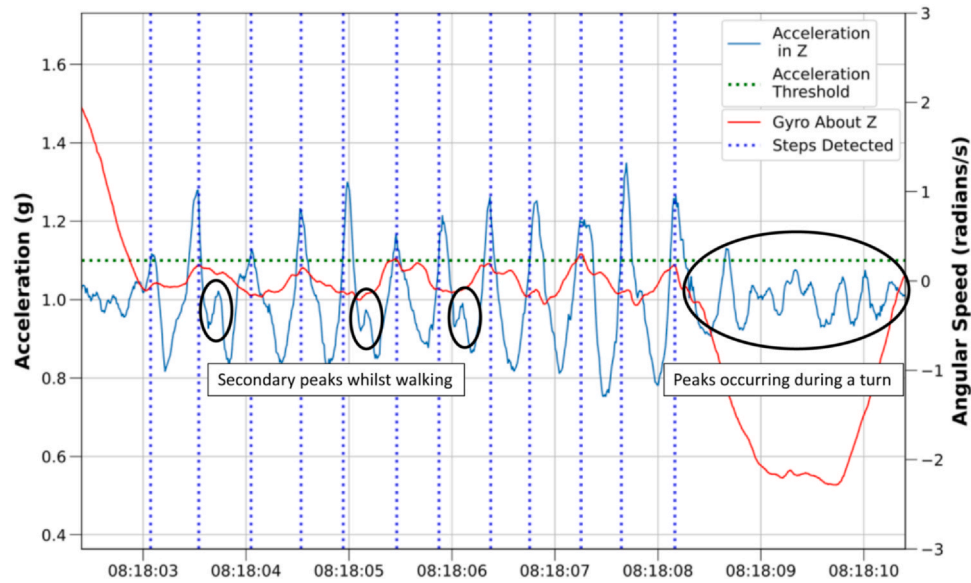


Fig. 9. Short timespan visualisation of step detection algorithm, highlighting secondary peaks whilst walking and repeated peaks during a turn.

Given the 1.5 m window resulting from the adoption of a RSSI threshold = 5000, at least 3 readings should be taken whilst walking past the tag at this pace in a worst-case scenario. In addition, rearranging Equation 3 it can also be shown that, to ensure a single reading is taken in the 1.5 m window, the maximum traveling speed of the person and the box must be $\leq 3.6 \text{ ms}^{-1}$ as shown in Equation 4.

$$\text{Max walking speed} = \frac{\text{Distance}}{\text{Sample Rate}} = \frac{1.5}{0.42} = 3.6 \text{ ms}^{-1} \quad (4)$$

The theoretical maximum speed is hence double the average walking speed of 1.4 m/s which indicates the viability of the approach.

From the unprocessed sensor measurements taken from the IMU, individual steps could be identified by features in the Z-axis acceleration as found in [21], combined with the gyroscopic motion about the Z axis (see Fig. 9). A step detection algorithm is used to analyse

the acceleration data collected by the IMU to identify when steps occur. This algorithm uses an acceleration threshold value (i.e. 1.1 g) on the Z-axis above which *turning points* are detected. These *turning points* are further classified such that only one turning point can occur within a 0.5 s window to reduce the impact of secondary peaks. In addition, steps that were correlated with large changes in gyroscopic motion were also eliminated from distance calculations as steps undertaken within a turn do not add to distance travelled. The performance of the step detection functionality is shown in Fig. 9 which present the number of steps detected using vertical blue dotted lines given the acceleration and gyroscopic motion input to the algorithm.

It can be seen in Fig. 9, that a simple peak detection algorithm would not be sufficient in determining the location of each step as several secondary peaks occur during walking whilst carrying boxes and when rotating see Fig. 9. The algorithm used to detect steps is presented as script written in Python 3 [61] below. The step detection algorithm was initiated each time a new RFID tag is detected to determine the positional changes between each tag read event.

This algorithm is a reliable indicator of the number of steps taken with a regular stride, detecting 116 steps in a test consisting of 120 steps, however it should be noted an additional 3 steps were identified upon pickup of the box, so the total step detection effectiveness is 94%. Using the method outlined in this paper missing steps becomes less of an issue in determining location as the RFID tags are used to update the current position. Should the step detection become insufficient in extended tests, a more complex algorithm could be utilised to detect features indicating a step, similar to the trained long short-term memory neural network which was accurately used to detect features of zero velocity conditions in [62].

Once the steps have been detected, the location of the box from the inertial navigation system (INS) is determined using step length of $0.75 \pm 0.05 \text{ m}$. The heading is calculated by rotating a vector initially pointing in the Y direction and applying the quaternion obtained using Madgwick's algorithm [26].

Integrated RFID tag update system evaluation

Using the hardware as illustrated in Fig. 7, an initial trial was conducted in which a 10 m length of corridor was tracked forwards and backwards, rotating 180° between lengths. The trial consisted of

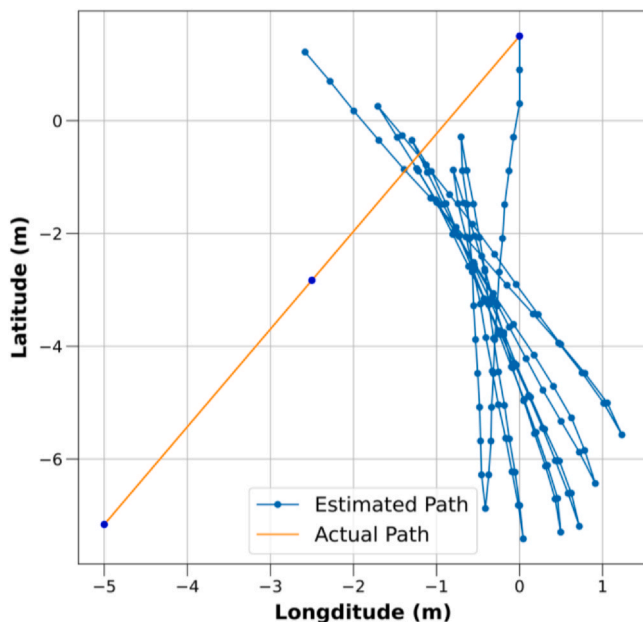


Fig. 10. Strap-down location with heading from Madgwick Algorithm.

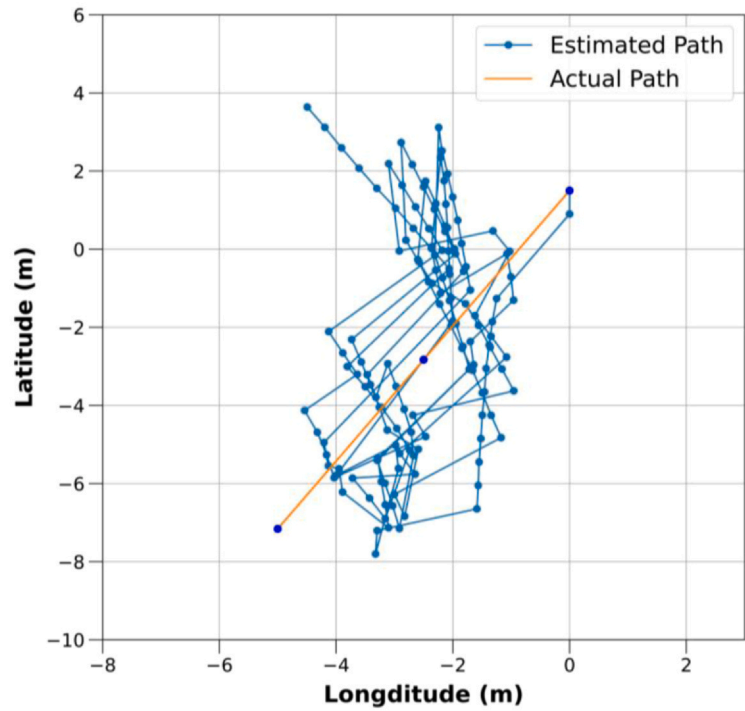
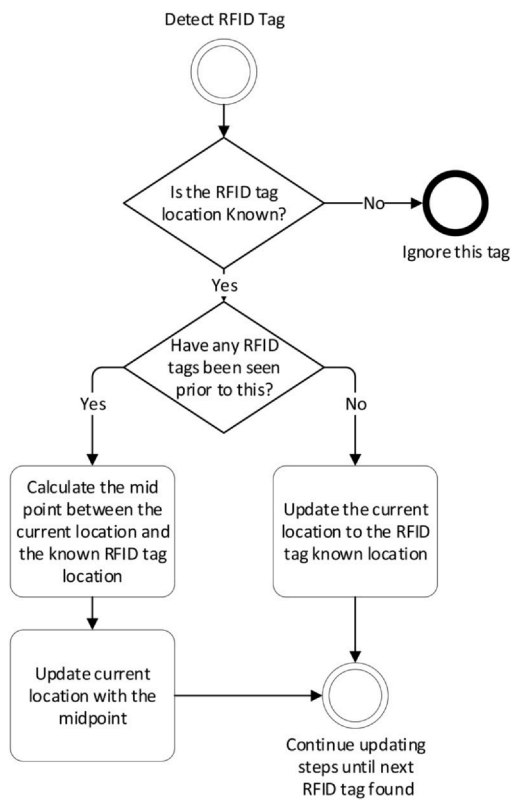


Fig. 11. RFID location update function process flow (left) and resulting path (right).

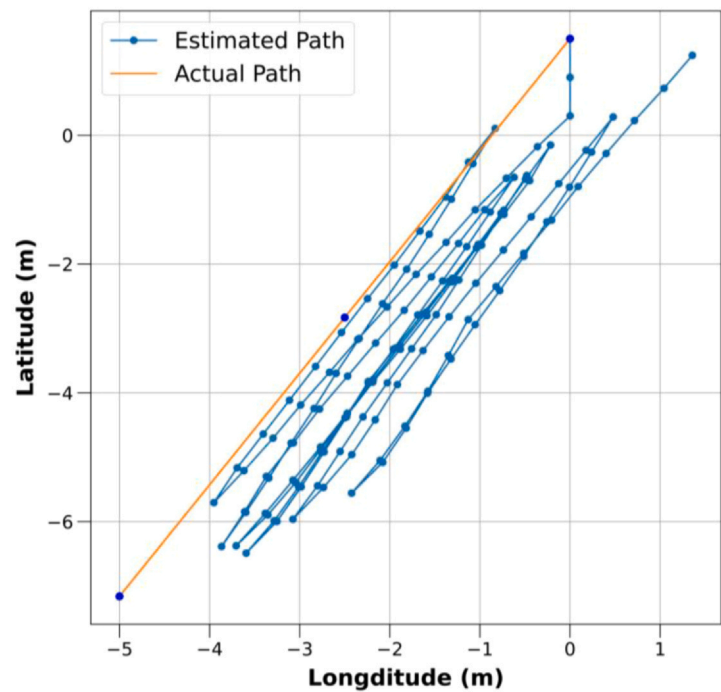
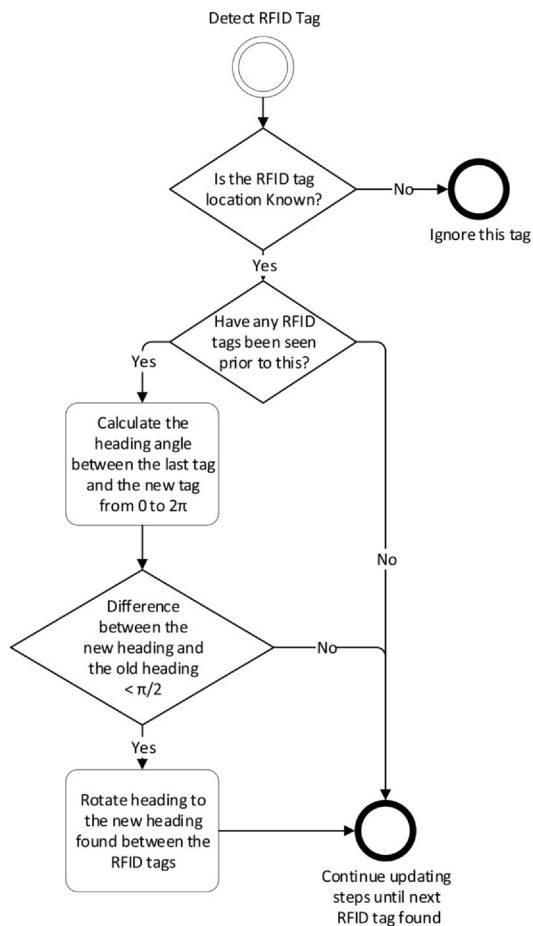


Fig. 12. RFID heading update function process flow (left) and resulting path (right).

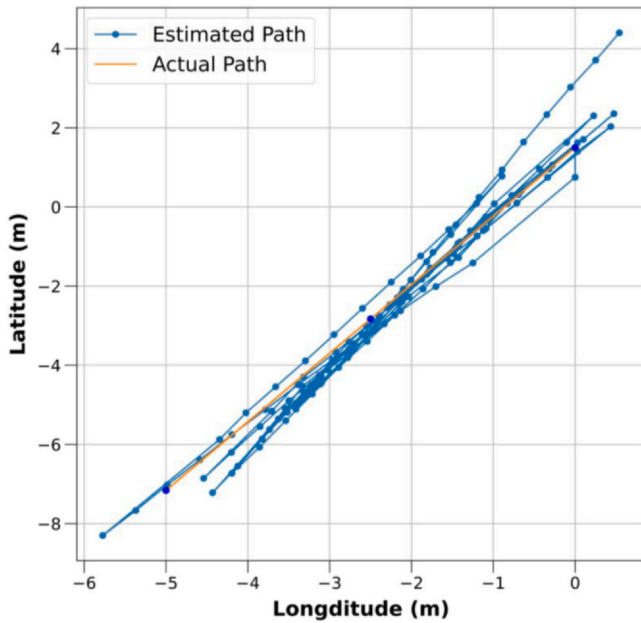


Fig. 13. Resulting path (right) from actual location over the distance travelled during combined Strap-down location estimation approach.

walking the 10 m length for a total of 6 repetitions (12 lengths) in a straight line, down the centre of the corridor, rotating 180° left at 0 m and right at 10 m. RFID tags were positioned along the walls either side of a corridor at 0 m, 5 m and 10 m, using these locations as the known ground truth. Throughout the test, acceleration and angular speed were recorded to be able to apply the *Strap-Down* algorithm, in addition to utilising the RSSI of all surrounding tags determined by the portable antenna / reader system. A threshold of 5000 was applied to the recorded RSSI to reduce the number of erroneous readings due to reflections within the corridor (typically 33% of the maximum signal recorded). In addition, the time of the maximum and the absolute value of each RSSI peak was taken to determine the most probable timestamp of passing specific locations. This approach measured the baseline “known” positions with a margin of error of approximately 0.75 m at 3 standard deviations as determined in Section V. The results of these tests have been summarised and presented in Section VIII-B.

To measure how well the predicted model matched the “known” RFID path, the results were analysed for mean error of location values using Eq. (5) where y_{pred} & x_{pred} denotes the predicted location of the algorithm and y & x denotes the “actual” path taken between the furthest RFID tags with 13 steps taken in each direction.

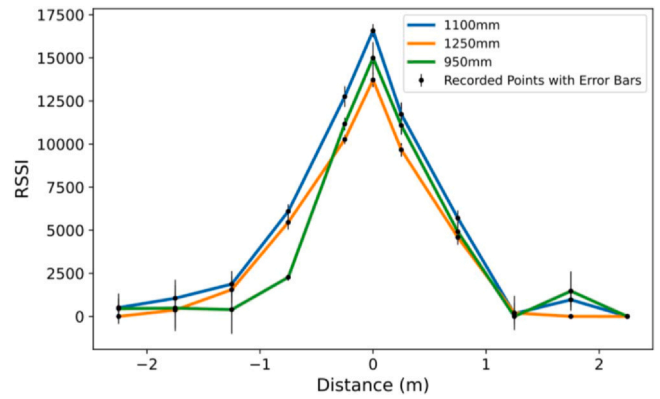


Fig. 15. Average RSSI from 60 readings at varying distances with an antenna perpendicular to the tag showing 3σ error bars.

$$\text{Mean Error} = \frac{\sum_{i=1}^n \left((x_{pred i} - x_i)^2 + (y_{pred i} - y_i)^2 \right)^{\frac{1}{2}}}{\text{steps}} \quad (5)$$

As an initial baseline, the *Strap-Down* approach using integrated Gyroscope response (Blue) was plotted against the ground truth (Orange) in Fig. 15. It can be seen in the diagram that as the initial heading is unknown from the gyroscope, the path is out of alignment with the actual motion. Furthermore, inaccuracy in the gyroscope angle calculation leads to an underestimate of angle rotated through at each turn (up to 5°), this further increases the deviation from the straight-line path walked shown in Fig. 10. The mean location distance error for this approach is 3.55 ± 1.58 m showing a poor accuracy.

Two approaches were adopted to reduce this error in position. Firstly, the location was updated as the midpoint between the known RFID location and the location determined by the *Strap-Down* algorithm. The *Strap-Down* approach would always need initialisation as mentioned previously, therefore the algorithm applies a 100% location weighting to the first tag found, updating the location as the midpoint between the *Strap-Down* heading prediction and the RFID location position thereafter the function process flow is given in Fig. 11. (left) This was found to have the effect of improving the location drift between the RFID tags, thus improving the overall location error and standard deviation to 1.89 ± 0.92 m however, this was unable to correct the error in initial heading as explained previously. The second approach is to update the heading when a number of tags are been found by updating the heading with the difference between the last two known tag locations the function



Fig. 14. Mapped path on building floorplan with updated location from RFID tags over a 65 m Track (known locations i.e. tag placements are depicted by red circles).

Table 3
Results of the tag orientation testing.

Orientation	RSSI
0°	3201
90°	621
180°	2074
270°	645

operations are given in Fig. 12. (left) This was found to improve the alignment of the path with the corridor and thus reduce the average and standard deviation to 2.0 ± 1.1 m however it did not account for the *Strap-Down* drift that occurs between RFID tag sightings and rotation underestimate, as a result the path is offset to the right of the expected path (see Fig. 12. (right)).

As both approaches were found to improve different aspects of the location with heading correction having the greatest impact, the heading update and location update algorithm were integrated with the *Strap-Down* approach applied to the accelerometers. This allowed for correction of the initial heading to align with the corridor and correct for the heading drift between RFID locations. The resulting tracked position can be seen in Fig. 13. This path estimation follows the “actual” path accurately after the recording of several consecutive tags, yielding a mean error of 0.97 ± 0.69 m, confirming the improved path fit when updated with the known RFID locations. Inspection of the data suggests the estimation of 0.75 m per stride was an accurate fit given the total distance travelled of 120.8 m and the expected path length of 120 m. Based on the visual representation of the path undertaken in Fig. 13 the path predicted closely follows the “actual” path travelled. It is noted that since the estimation of the total distance travelled is greater than that of the distance between tags, correctly estimating average stride length was not critical with frequent RFID sightings and meant that the proposed system could compensate for variable stride length within/between persons.

To simulate an industrial environment, a longer test was conducted with a 65 m route of an along the corridor with multiple interferences such as a metallic stairwell, and rooms with operational computers. Results are summarised in Section VIII – C. Two RFID tags were positioned at the start of the route to align the initial path estimation and avoid early drift due to no heading information. The predicted route on the floorplan is given in map view of this test can be seen in Fig. 14. The predicted path (blue) follows the approximate known route recorded at intervals with floor markings (Red Dots). It is noted that the path travelled near the stairwell (Stair 7) has an increased location error. This is possibly due to the highly metallic structure in the stairwell or possibly due to tags being located near wire mesh glass. Either of these influences may have led to RFID readings occurring earlier or later than expected, in addition the error continues to increase after this point as no other tags were available to correct the drift. The tags in this test were set 20 m apart which may have been too large a distance leading to the continual drift and then correction seen in the error shown in Fig. 17. The optimal distance between reference tags is a trade-off between positional resolution required and cost, however, the approach using RFID tags has improved the location estimation by yielding an

Table 4
Results of the FWHM and rise and fall time calculations for the perpendicular offset of tags.

Tag Height	FWHM	Rise Time	Fall Time
1250 mm	0.869 m	1.273	0.799
1100 mm	0.879 m	1.226	0.799
950 mm	1.003 m	1.143	0.807
Average	0.917 ± 0.061	1.214 ± 0.054	0.802 ± 0.004

improved heading and location once two tags have been observed. Following this the algorithm has improved alignment with a maximum error of 7.6 m, mean error of 3 m and final location error of 0.9 m.

Results and discussion

RFID tag testing results

The results from the RFID tag rotation test indicate that values of RSSI varied by 80% and were a minimum when oriented perpendicular to the antenna (i.e. 90° and 270°), the results of these tests are summarised in Table 2.

In the vertical offset test (the antenna was moved past the tags' locations), an average RSSI of 16573 was recorded when in line with tag which fell with increase in the lateral offset from the tag, see Fig. 15. The results suggest that readings were strongest (i.e. RSSI > 5000) within a 0.75 m range of the tag. The full width half maximum (FWHM), rise time and fall time calculation results are shown in Table 3.

In addition, the variability of readings when the antenna offset was ≤ 0.75 m were small, yielding a maximum standard deviation for the tag at 950 mm, of 307.2 (i.e. 2%) when in line with the tag (i.e. at position 0 m). Overall, the height variation had very little impact on the signals received with respect to the full width half maximum (FWHM), with the largest impact being the lower tag, increasing the FWHM by 0.124 m from the central tag (14%). The position determined from walking past an RFID tag was however considered as a binary classifier in terms of an output of *detected* vs *not detected* via implementing a lower threshold of 5000 units of RSSI, utilising the steepest section of the slope.

RFID update algorithm short repeated 10 m track evaluation route

The results for the RFID update algorithm development tests, are summarised in Table 4. The predicted location error is plotted against distance travelled in Fig. 16. The path with no heading information showed the largest error and standard deviation (3.55 ± 1.58 m). Each of the techniques of updating the path location and the heading individually resulted in an improvement of the mean error by 1.66 m and 1.55 m respectively.

Fig. 16 shows a cyclical error increase over the 10 m path, these cycles coincide with the 180° turn as the error in heading produced the largest source of inaccuracy in the original path. This cyclical nature was reduced when the combined heading and location update of the RFID tags was applied, reducing the standard deviation from 1.58 m to 0.69 m.

Final RFID update algorithm extended 75 m evaluation route

The final algorithm evaluation test was conducted on 65 m route along an internal corridor with multiple interference effects. The location error for this test is presented as a function of the distance in Fig. 17. The location error increased (see Table 5) from path between 34 m and 44 m to a maximum of 7.6 m at 38 m.

The algorithm yields location and path alignment with a minimum error of 0.26 m, a maximum error of 7.6 m which occurred at 38 m, mean error of 3 m and final location error of 0.9 m. This mean error for the 65 m route is increased when compared with the repeated shorter 10 m path, however the final location lies within the mean error of the algorithm. These results suggest that the algorithm recovers after a loss of location accuracy once additional tags are detected (Table 6).

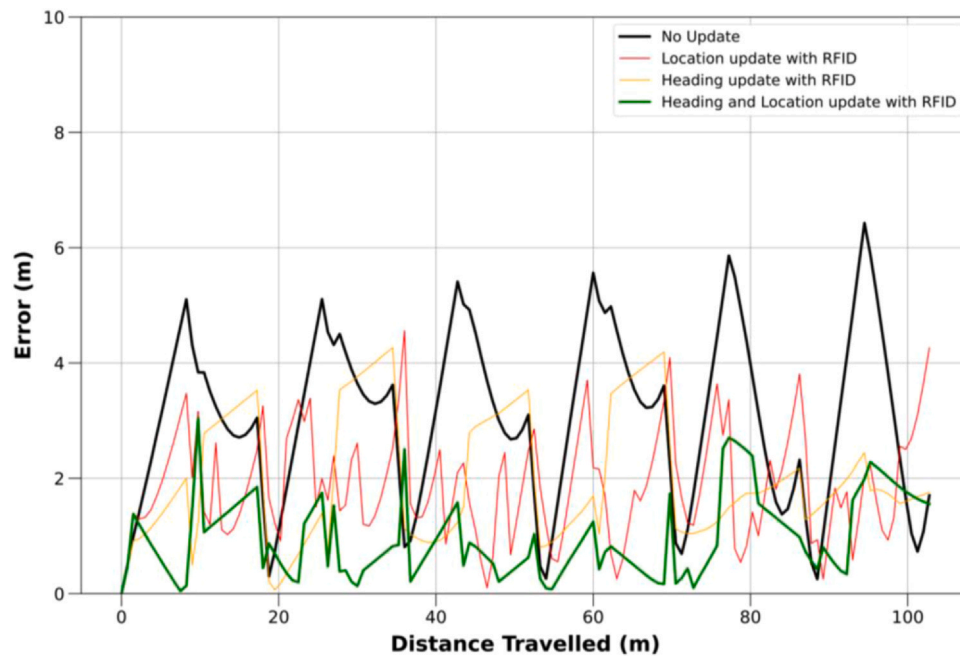


Fig. 16. Evolution of estimated error from actual location over the distance travelled for the repeated 10 m track for each approach.

Limitations, implications for practitioners and further work

The research presented in this paper demonstrates the development of a system utilising low cost, low infrastructure impact technologies to provide accurate tracking of assets when carried by personnel in indoor environments including those with interference. The results outlined in this paper demonstrate the promising approach to improve the *Strap-Down* technique that has been applied in other studies [9,46]. In addition, the EPC values of each tag can be used to relate individual readings to a known position in a real-world map, linking the path to an accurate position in the real world.

Table 5

Summary of the error found for the repeated 10 m walk test for each analysis technique.

Technique	Mean Error (m)	Error Standard Deviation (m)
No RFID input	3.55	1.58
RFID to update location	1.89	0.92
RFID to update heading	2.0	1.1
RFID to update location and heading	0.97	0.69

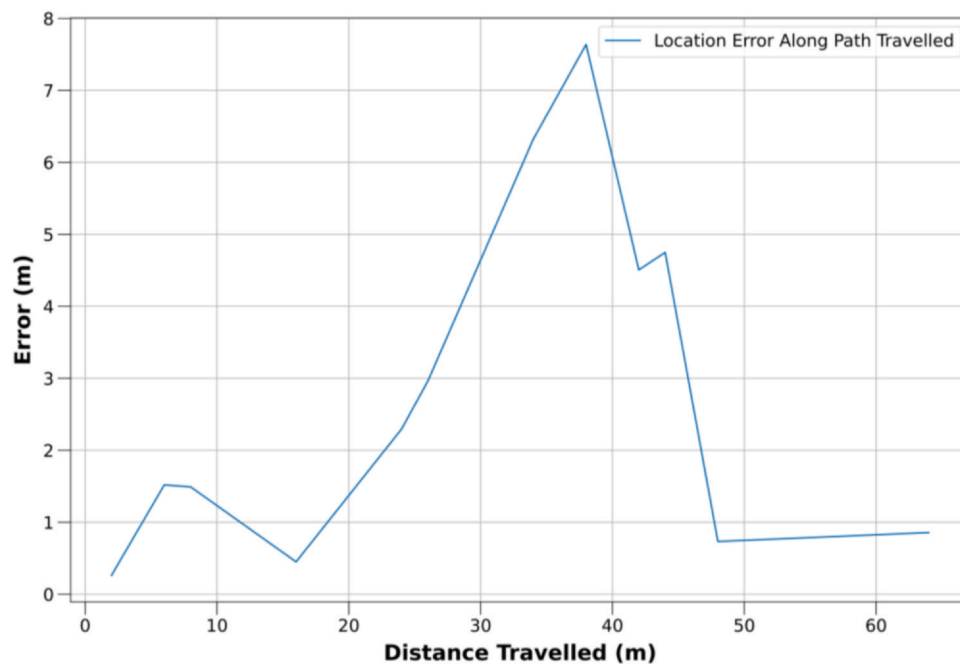


Fig. 17. Evolution of estimated error from actual location over the distance travelled for the 65 m track.

Table 6

Known locations and corresponding predicted location at this point with resulting location error in meters.

X (m)	Y (m)	X Predicted (m)	Y Predicted (m)	Magnitude Error (m)
2.00	0.80	2.24	0.70	0.26
6.00	0.80	4.49	0.64	1.52
8.00	0.80	6.70	0.07	1.49
16.00	0.80	16.45	0.80	0.45
24.00	0.80	22.70	-1.09	2.29
26.00	0.80	23.17	-0.07	2.96
34.00	0.80	27.68	0.92	6.32
38.00	0.80	30.39	0.17	7.64
42.00	0.80	37.50	0.66	4.51
44.00	0.80	39.26	0.58	4.75
48.00	0.80	47.28	0.69	0.73
64.00	0.80	64.65	1.36	0.86

There are a number of limitations that will be addressed through the iterative refinement of the system. However, the novel findings of the reported testing contribute to the refinement of IPS system development in general. In addition, the protocol for evaluation and analysis provide several successful techniques for use in further research and academia. The improved *Strap-Down* technique with updated positioning based on short range (i.e. < 10 m) passive RFID tags has thus far been tested with an indoor corridor scenario which resulted in errors of 0.97 ± 0.69 m. However, a significant limitation was that this value deviated when stride estimation was incorrect for the individual using the system. To remove this error, an accurate individual stride length would need to be input or calculated by the system during a configuration phase, prior to position and path estimation. One example method would be to calculate average stride length using the number of strides between two tags. An additional limitation of the step and heading technique is that 3 'steps' were identified when the unit was picked up, this may lead to inaccuracies for interrupted paths where the user places the container down for a rest for example. Further work will be needed to refine the step detection algorithm and test how the system responds to intermittent pauses on route.

The use of passive RFID tags was evaluated as an inexpensive infrastructural addition to update the heading and location of an IMU based location system is a novel approach for scenarios in which the use of zero velocity conditions and magnetometer heading are not possible. Unfortunately, commercial RFID reader systems are currently expensive (i.e. >£100 per system, primarily due to the reader cost) for use cases when transporting low value goods. The system was developed as a proof-of-concept system and smaller form factor equipment with lower power consumption would need to be sourced for future iterations to make the system more practical for use in industry. The proposed approach could support practitioners in utilising combined methods to ensure traceability of assets with more accuracy and less cost to implement. Although the proposed system was not as low cost as possible, this was a necessary compromise to ensure accuracy. For practitioners, this is an important consideration due to the introduction of GDPR, the cost of loss of data carrying media could incur fines of up to €20 million [63] and should be included in system cost evaluation. A system such as the one proposed may be a justifiable cost when compared with the financial risk of data loss. However, there are limited pilot studies revealing the benefits of this risk mitigation approach within industrial settings and further work is needed to clarify return on investment, especially for small / medium enterprise [1]. In addition to the cost of the system, further work will be needed to reduce the size of the components, at current the prototype uses components which are heavy and have a large package volume, this will increase load and detrimentally impact manual handling performance. A possible avenue would be to replace the RFID reader with a smaller device, such as the Thingmagic

M6E-NANO [64], which would greatly reduce the weight of the system and reduce the power requirements, allowing a smaller battery to be used. Acceptable weight, package volume and device fixture requirements for industrial application are still to be explored.

Further work will include testing the accuracy on more complex building areas and in larger open spaces and over multiple floors. In the 65 m test it was noted that the optimal position of the reference tags needs refinement, future work will determine the optimum placement of each tag with respect to other tags and surrounding materials whilst reducing the length of the initial, non-oriented path. Further work on the system will introduce redundancy by utilising other opportune signals such as Wi-Fi or Bluetooth beacon locations within a building where available to allow orientation if the RFID signals are compromised (i.e. in close proximity to metal objects). A drawback of the current system is that the RFID tags must be manually assigned to their positions, further work could utilise the tag EPC to write the location allowing the reader to automatically determine its location in real time. Further to this, the system currently utilises recorded data to calculate path and location estimation. Future work will investigate developing the system such that location updates are based on real-time measurements sent to a local server and displayed to the user using a user interface.

Declaration of Competing Interest

The authors declare that they have no known competing financial interests or personal relationships that could have appeared to influence the work reported in this paper.

Acknowledgment

The authors gratefully acknowledge the financial support of the UK Engineering and Physical Sciences Research Council (EPSRC) Centre for Doctoral Training in Embedded Intelligence under grant reference EP/L014998/1 and S2S Electronics for their support and input to this research.

References

- [1] Segura Velandia, D.M., Kaur, N., Whittow, W.G., Conway, P.P., West, A.A., 2016, Towards Industrial Internet of Things: Crankshaft Monitoring, Traceability and Tracking using RFID. *Robotics and Computer-Integrated Manufacturing*, 41:66–77. <https://doi.org/10.1016/j.rcim.2016.02.004>. (Oct.).
- [2] Deutsche, H., Henning, P.A. Kagermann (National Academy of Science and Engineering). Wolfgang, Wahlster (German Research Center for Artificial Intelligence). Johannes, "Recommendations for implementing the strategic initiative INDUSTRIE 4.0," Final Rep. Ind. 4.0 WG, no. April, 2013, p. 82, doi: 10.13140/RG.2.1.1205.8966.
- [3] N. Papakostas, J. O'Connor, G. Byrne, Internet of Things Technologies in Manufacturing: Application Areas, Challenges and Outlook, in: *International Conference on Information Society, i-Society 2016*, Oct. 2017, pp. 126–131, doi: 10.1109/i-Society.2016.7854194.
- [4] Huang, H., Gartner, G., Krisp, J.M., Raubal, M., Van de Weghe, N., 2018, Location Based Services: Ongoing Evolution and Research Agenda. *The Journal of Location Based Services*, 12/2: 63–93. <https://doi.org/10.1080/17489725.2018.1508763>.
- [5] Raj, A., Dwivedi, G., Sharma, A., Lopes de Sousa Jabbour, A.B., Rajak, S., 2020, Barriers to the Adoption of Industry 4.0 Technologies in the Manufacturing Sector: An Inter-Country Comparative Perspective. *International Journal of Production Economics*, 224:107546 <https://doi.org/10.1016/j.ijpe.2019.107546>. (Jun.).
- [6] D. Newman, 5 IoT Trends To Watch In 2021, Forbes, 2020. <https://www.forbes.com/sites/danielnewman/2020/11/25/5-iot-trends-to-watch-in-2021/?sh=27c79dc201b3> (Accessed Jul. 14, 2021).
- [7] S. Saha, S. Chatterjee, A.K. Gupta, I. Bhattacharya, T. Mondal, TrackMe - A Low Power Location Tracking System using Smart Phone Sensors, in: *2015 International Conference on Computing and Network Communications (CoCoNet)*, Dec. 2015, pp. 457–464, doi: 10.1109/CoCoNet.2015.7411226.
- [8] Kim Geok, T., Zar Aung, K., Sandar Aung, M., Thu Soe, M., Abdaziz, A., Pao Liew, C., Hossain, F., Tso, C.P., Yong, W.H., 2020, Review of Indoor Positioning: Radio Wave Technology. *Applied Sciences*, 11/1: 279. <https://doi.org/10.3390/app11010279>. (Dec.).
- [9] Correa, A., Barcelo, M., Morell, A., Vicario, J.L., 2017, A Review of Pedestrian Indoor Positioning Systems for Mass Market Applications. *Sensors*

- Multidisciplinary Digital Publishing Institute, Switzerland: 1927. <https://doi.org/10.3390/s17081927>. (Aug. 22).
- [10] S. Deng, T. Fan, W. He, Analysis the Impact of the RFID Technology on Reducing Inventory Shrinkage, in: Proceedings - 2010 International Conference on Optoelectronics and Image Processing, ICOIP 2010, Nov. 2010, vol. 1, pp. 267–270, doi: [10.1109/ICOIP.2010.134](https://doi.org/10.1109/ICOIP.2010.134).
 - [11] Rekkik, Y., Sahin, E., Dallery, Y., 2009, Inventory Inaccuracy in Retail Stores due to Theft: An Analysis of the Benefits of RFID. *International Journal of Production Economics*, 118/1: 189–198. <https://doi.org/10.1016/j.ijpe.2008.08.048>.
 - [12] Kelepouris, T., McFarlane, D., 2010, Determining the Value of Asset Location Information Systems in a Manufacturing Environment. *International Journal of Production Economics*, 126:324–334. <https://doi.org/10.1016/j.ijpe.2010.04.009>.
 - [13] Daniel Bastos, Fabio Giubilo, Mark Shackleton, Fadi El-Mousa, GDPR Privacy Implications for the Internet of Things, in: 4th Annual IoT Security Foundation Conference, Dec. 2018, Accessed: May 26, 2021. [Online]. Available: (https://www.researchgate.net/publication/331991225_GDPR_Privacy_Implications_for_the_Internet_of_Things).
 - [14] The European Parliament and the Council of the European Union, General Data Protection Regulation, 2016, p. 88.
 - [15] (www.eugdpr.org), Key Changes with the General Data Protection Regulation, 2018. (<https://www.eugdpr.org/key-changes.html>) (Accessed Mar. 07, 2018).
 - [16] N. Strozzi, F. Parisi, G. Errari, A Novel Step Detection and Step Length Estimation Algorithm for Hand-held Smartphones, in: International Conference on Indoor Positioning and Indoor Navigation (IPIN), Sep. 2018, no. September, pp. 24–27, doi: [10.1109/IPIN.2018.8533807](https://doi.org/10.1109/IPIN.2018.8533807).
 - [17] Obeidat, H., Shuaib, W., Obeidat, O., Abd-Alhameed, R., 2021, A Review of Indoor Localization Techniques and Wireless Technologies. *Wireless Personal Communications*. Springer: 1–39. <https://doi.org/10.1007/s11277-021-08209-5>. (Feb. 19).
 - [18] Yoon, Y.-J., Li, K.H.H., Lee, J.S., Park, W.-T., 2015, Real-time precision pedestrian navigation solution using inertial navigation system and global positioning system. *Advances in Mechanical Engineering*, 7/3: 371. <https://doi.org/10.1177/1687814015568501>. (Mar.) (1687814015568501).
 - [19] Bojja, J., Kirkko-Jaakkola, M., Collin, J., Takala, J., 2013, Indoor Localization Methods Using Dead Reckoning and 3D Map Matching. *The Journal of Signal Processing Systems*, 76/3: 1–12. <https://doi.org/10.1007/s11265-013-0865-9>. (Sep.).
 - [20] Prime Faraday Partnership Loughborough University, Prime Faraday Technology Watch An Introduction to MEMS (Micro-electromechanical Systems), An Intro. to MEMS (Micro-electromechanical Syst., 2002. [Online]. Available: (<http://www.amazon.co.uk/exec/obidos/ASIN/1844020207>). (Accessed: May 15, 2020).
 - [21] Sharp, I., Yu, K., 2014, Sensor-Based Dead-Reckoning for Indoor Positioning. *Physics Communications*, 13/PA: 4–16. <https://doi.org/10.1016/j.phycom.2013.11.013>. (Dec.).
 - [22] X. Chen, S. Song, J. Xing, A ToA/IMU Indoor Positioning System by Extended Kalman Filter, Particle Filter and MAP Algorithms, in: 2016 IEEE 27th Annual International Symposium on Personal, Indoor, and Mobile Radio Communications (PIMRC), Sep. 2016, pp. 1–7, doi: [10.1109/PIMRC.2016.7794980](https://doi.org/10.1109/PIMRC.2016.7794980).
 - [23] A.R. Jimenez, F. Seco, P. Peltola, M. Espinilla, Location of Persons Using Binary Sensors and BLE Beacons for Ambient Assisted Living, in: 2018 International Conference on Indoor Positioning and Indoor Navigation (IPIN), Sep. 2018, no. September, pp. 206–212, doi: [10.1109/IPIN.2018.8533714](https://doi.org/10.1109/IPIN.2018.8533714).
 - [24] Ong, S.K., Yuan, M.L., Nee, A.Y.C., 2008, Augmented Reality Applications in Manufacturing: A Survey. *International Journal of Production Research*, 46/10: 2707–2742. <https://doi.org/10.1080/00207540601064773>.
 - [25] Kok, M., Hol, J.D., Schön, T.B., 2017, Using Inertial Sensors for Position and Orientation Estimation. *Foundations and Trends in Signal Processing*, 11/1–2: 1–153. <https://doi.org/10.1561/20000000094>.
 - [26] S.O. H. Madgwick, An Efficient Orientation Filter for Inertial and Inertial/Magnetic Sensor Arrays, 2010. [Online]. Available: (https://www.x-io.co.uk/res/doc/madgwick_internal_report.pdf). (Accessed: May 19, 2020).
 - [27] M. Henriksson, Estimation of Heading using Magnetometer and GPS, no. September, 2013. [Online]. Available: (<https://www.semanticscholar.org/paper/Estimation-of-heading-using-magnetometer-and-GPS-Henriksson/98f35084669a7d3926ea96e21e9389c1ce51661c>). (Accessed: May 21, 2020).
 - [28] Pirker, W., Katzenschlager, R., 2017, Gait Disorders in Adults and the Elderly: A Clinical Guide. *Wiener klinische Wochenschrift*, 129/3–4: 81–95. <https://doi.org/10.1007/s00508-016-1096-4>. (Feb.).
 - [29] J. Haverinen and A. Kemppainen, A Global Self-Localization Technique Utilizing Local Anomalies of the Ambient Magnetic Field, in: Proceedings - IEEE International Conference on Robotics and Automation, May 2009, pp. 3142–3147, doi: [10.1109/ROBOT.2009.5152885](https://doi.org/10.1109/ROBOT.2009.5152885).
 - [30] Chen, Y., Zhou, M., Zheng, Z., 2019, Learning Sequence-Based Fingerprint for Magnetic Indoor Positioning System. *IEEE Access*, 7:163231–163244. <https://doi.org/10.1109/ACCESS.2019.2952564>.
 - [31] Kárník, J., Streit, J., 2016, Summary of Available Indoor Location Techniques. *IFAC-PapersOnLine*, 49/25: 311–317. <https://doi.org/10.1016/j.ifacol.2016.12.055>. (Jan.).
 - [32] Tahir, M.A., Ferrer, B.R., Lastra, J.L.M., 2019, An Approach for Managing Manufacturing Assets through Radio Frequency Energy Harvesting. *Sensors*, 19/3: 438. <https://doi.org/10.3390/S19030438>.
 - [33] Baha Aldin, N., Ercelebi, E., Aykaç, M., 2017, An Accurate Indoor RSSI Localization Algorithm Based on Active RFID System with Reference Tags. *Wireless Personal Communications*, 97/3: 3811–3829. <https://doi.org/10.1007/s11277-017-4700-7>. (Dec.).
 - [34] M.E. Rusli, M. Ali, N. Jamil, M.M. Din, An Improved Indoor Positioning Algorithm Based on RSSI-Trilateration Technique for Internet of Things (IoT), in: 2016 International Conference on Computer and Communication Engineering (ICCE), Jul. 2016, pp. 72–77, doi: [10.1109/ICCE.2016.28](https://doi.org/10.1109/ICCE.2016.28).
 - [35] W. Bulten, A.C. Van Rossum, W.F. G. Haselager, Human SLAM, Indoor Localisation of Devices and Users, in: 2016 IEEE First International Conference on Internet-of-Things Design and Implementation (IoTDI), Apr. 2016, pp. 211–222, doi: [10.1109/IoTDI.2015.19](https://doi.org/10.1109/IoTDI.2015.19).
 - [36] Zou, Z., Chen, Q., Uysal, I., Zheng, L., 2014, Radio frequency identification enabled wireless sensing for intelligent food logistics. *Philosophical Transactions of The Royal Society A Mathematical Physical and Engineering Sciences*, 372/2017: 20130313. <https://doi.org/10.1098/rsta.2013.0313>. (Jun.) (20130313–20130313).
 - [37] RS, RS Components | Industrial, Electronic Products & Solutions, 2020. (https://uk.rs-online.com/web/?cm_mmc=World-Selector-Page-Online-ReferralMainWorldList-CountryList) (Accessed May 21, 2020).
 - [38] Deng, Z., Zheng, X., Zhang, C., Wang, H., Yin, L., Liu, W., 2020, A TDOA and PDR Fusion Method for 5G Indoor Localization Based on Virtual Base Stations in Unknown Areas. *IEEE Access*, 8:225123–225133. <https://doi.org/10.1109/ACCESS.2020.3044812>.
 - [39] Y. He, Z. Pan, Design of UHF RFID Broadband Anti-Metal Tag Antenna Applied on Surface of Metallic Objects, in: IEEE Wireless Communications and Networking Conference, WCNC, Apr. 2013, pp. 4352–4357, doi: [10.1109/WCNC.2013.6555278](https://doi.org/10.1109/WCNC.2013.6555278).
 - [40] A.R. J. Ruiz, F.S. Granja, J.C. P. Honorato, J.I. G. Rosas, Pedestrian Indoor Navigation by Aiding a Foot-Mounted IMU with RFID Signal Strength Measurements, in: 2010 International Conference on Indoor Positioning and Indoor Navigation, IPIN 2010 - Conference Proceedings, Sep. 2010, pp. 1–7, doi: [10.1109/IPIN.2010.5646885](https://doi.org/10.1109/IPIN.2010.5646885).
 - [41] A.T. Corporation, The Art and Science of UHF Passive Tag Design And Selecting The Tag That is Best for Your Requirements, 2013. [Online]. Available: (http://www.iso.org/iso/home/store/catalogue_ics/catalogue_detail_ics.htm?csnumber=59644). (Accessed: Jan. 08, 2019).
 - [42] T. Gujarathi, K. Bhole, GAIT ANALYSIS USING IMU SENSOR, in: 2019 10th International Conference on Computing, Communication and Networking Technologies, ICCNT 2019, Jul. 2019, pp. 1–5, doi: [10.1109/ICCCNT45670.2019.8944545](https://doi.org/10.1109/ICCCNT45670.2019.8944545).
 - [43] Alien Technology, ALN-9640 Squiggle Inlay, 2014. (https://www.rfidglobal.it/download/sales/datasheet_apparati_rfid/Transponder-RFID-Passivi/etichette_rfid_uhf_alien/ALN-9640_Squiggle_Higgs3_RFID_Global.pdf) (Accessed May 19, 2020).
 - [44] Potorti, F., Park, S., Jiménez Ruiz, A.R., Barsocchi, P., Girolami, M., Crivello, A., Lee, S.Y., Lim, J.H., Torres-Sospedra, J., Seco, F., Montoliu, R., Mendoza-Silva, G.M., Pérez Rubio, M., Losada-Gutiérrez, C., Espinosa, F., Macías-Guarasa, J., 2017, Comparing the Performance of Indoor Localization Systems through the EvAAL Framework. *Sensors*, 17/10: 2327. <https://doi.org/10.3390/s17102327>. (Oct.).
 - [45] He, S., Chan, S.H.G., 2016, Wi-Fi Fingerprint-Based Indoor Positioning: Recent Advances and Comparisons. *IEEE Communications Surveys and Tutorials*, vol. 18/1: 466–490. <https://doi.org/10.1109/COMST.2015.2464084>.
 - [46] Zafari, F., Gkelias, A., Leung, K.K., 2019, A Survey of Indoor Localization Systems and Technologies. *IEEE Communications Surveys and Tutorials*, 21/3: 2568–2599. <https://doi.org/10.1109/comst.2019.2911558>.
 - [47] F. Seco, A.R. Jiménez, P. Peltola, A Review of Multidimensional Scaling Techniques for RSS-Based WSN Localization, IPIN 2018 - 9th Int. Conf. Indoor Position. Indoor Navig., no. Fig. 1, 2018, doi: [10.1109/IPIN.2018.8533748](https://doi.org/10.1109/IPIN.2018.8533748).
 - [48] Basiri, A., Lohan, E.S., Moore, T., Winstanley, A., Peltola, P., Hill, C., Amirian, P., Figueiredo e Silva, P., 2017, Indoor Location Based Services Challenges, Requirements and Usability of Current Solutions. *Computer Science Review*, 24:1–12. <https://doi.org/10.1016/j.cosrev.2017.03.002>.
 - [49] Alarifi, A., Al-Salman, A., Alsaleh, M., Alnafessah, A., Al-Hadhrami, S., Al-Ammar, M.A., Al-Khalifa, H.S., 2016, Ultra Wideband Indoor Positioning Technologies: Analysis and Recent Advances. *Sensors*, 16:1–36. <https://doi.org/10.3390/s16050707>.
 - [50] Digi-Key, DigiKey Electronics United Kingdom, 2020. (<https://www.digikey.co.uk/>) (Accessed May 22, 2020).
 - [51] Symmetry Electronics, SymmetryElectronics.com, 2020. (<https://www.semiconductorstore.com/>) (accessed May 22, 2020).
 - [52] RFID Shop, RFID Readers and Tags - Available on-line and in Low Volumes at TheRFIDShop.com - RFID Readers and Tags, 2020. (<https://www.therfidshop.com/>) (Accessed May 22, 2020).
 - [53] Burhan, M., Rehman, R.A., Khan, B., Kim, B.S., 2018, IoT Elements, Layered Architectures and Security Issues: A Comprehensive Survey. *Sensors*, 18/9: 2796. <https://doi.org/10.3390/s18092796>. (Aug.).
 - [54] Han, K., Xing, H., Deng, Z., Du, Y., 2018, A RSSI/PDR-Based Probabilistic Position Selection Algorithm with NLOS Identification for Indoor Localisation. *ISPRS International Journal of Geo-Information*, 7/6: 232. <https://doi.org/10.3390/ijgi7060232>. (Jun.).
 - [55] espressif Systems, This Document Provides the Specifications for the ESP32-WROOM-32D and ESP32-WROOM-32U Modules, Espressif Systems, 2019. (www.espressif.com/en/subscribe). (Accessed May 15, 2020).
 - [56] RASPBERRY PI FOUNDATION, Buy a Raspberry Pi 3 Model B+ - Raspberry Pi, 2018. (<https://www.raspberrypi.org/products/raspberry-pi-3-model-b-plus/>) (Accessed May 15, 2020).
 - [57] Alien, ALR-8696-C Low VSWR/Axial Ratio Antenna, 2011. [Online]. Available: (www.alientechnology.com). (Accessed: May 18, 2020).
 - [58] Alien, ALR 9900+ Datasheet (2015 09 17), ALR 9900+ Datasheet (2015 09 17), 2015. (<https://www.alientechnology.com/products/files-2/alr-9900/>) (Accessed May 15, 2020).

- [59] Health and Safety Executive, Health and Safety Executive Manual Handling Assessment - Charts (the MAC tool), 2016, pp. 1–20. [Online]. Available: www.hse.gov.uk/msd/mac/scoresheet.htm. (Accessed: Jan. 10, 2020).
- [60] Pheasant, S., 1996, *Bodyspace: Anthropometry, Ergonomics, and the Design of Work*. Taylor & Francis.
- [61] Python, Python 3.0 Release | Python.org. Python, 2019. [Online]. Available: <https://www.python.org/download/releases/3.0/>. (Accessed: May 15, 2020).
- [62] Wagstaff, B., Peretroukhin, V., Kelly, J., 2020, Robust Data-Driven Zero-Velocity Detection for Foot-Mounted Inertial Navigation. *IEEE Sensors Journal*, 20/2: 957–967. <https://doi.org/10.1109/JSEN.2019.2944412>. (Jan.).
- [63] Legislation UK, Data Protection Act 2018 Explanatory Notes, no. May. London, 2018, p. 340.
- [64] JADAK, OEM Embedded ThingMagic UHF/RAIN RFID Module / Nano | JADAK, 2021. <https://www.jadaktech.com/products/thingmagic-rfid/thingmagic-m6e-nano-uhf-rain-rfid/#spec-sheets> (Accessed Jul. 14, 2021).